



## **Comparative Analysis of Voltage Output in Piezoelectric Sensors for Energy Harvesting Applications**

Jared Baza  
Del Norte High School  
November 21, 2025

### Abstract

Piezoelectric materials offer promising solutions for sustainable energy harvesting by converting mechanical deformation into electrical energy. This study investigates the voltage output characteristics of three piezoelectric sensor types — 12 mm ceramic discs, 35 mm ceramic discs, and flexible PVDF film — under controlled impact conditions at drop heights of 3, 6, 9, and 12 cm using a 2.7 kg mass. An Arduino Uno R3 captured voltage outputs across repeated trials to assess performance, repeatability, and reliability. Results demonstrated that the 12 mm disc achieved the highest voltages at high impact forces, the 35 mm disc showed the greatest sensitivity at moderate energies, and the PVDF film demonstrated the most linear response and the highest consistency across all conditions. Statistical analysis confirmed that observed differences exceeded measurement uncertainty, with coefficients of variation below 10%. These findings indicate that sensor selection should be matched to application requirements: 12 mm discs for high-energy impact detection, 35 mm discs for moderate-force energy harvesting, and PVDF films for flexible, motion-sensitive systems. This work contributes to the optimization of piezoelectric sensor design for self-powered devices and wearable electronics.

*Keywords:* Piezoelectric sensor, energy harvesting, ceramic disks, PVDF film, Arduino, self-powered devices, wearable electronics

## Introduction

### Motivation and Background

The rapid expansion of portable electronics and wireless sensor systems has intensified demand for sustainable, maintenance-free power sources (Priya & Inman, 2007). Conventional batteries impose constraints on longevity, cost, and environmental impact (Tarascon & Armand, 2001), making self-sustaining energy systems a growing field of investigation and technological development. One promising solution involves piezoelectric materials, which convert mechanical deformation directly into electrical energy through the piezoelectric effect. These materials enable energy harvesting from ordinary vibrations, pressure, or motion, offering potential applications across personal, industrial, and municipal scales (Anton & Sodano, 2007; Goldschmidt et al., 2009; Khaligh et al., 2009; Erturk & Inman, 2011).

Piezoelectric energy harvesting has been proposed for integration in environments where mechanical input is abundant but typically wasted. Embedding piezoelectric elements beneath flooring, roadways, or rail lines would enable continuous conversion of human or vehicular motion into usable electrical power (Lawman et al., 2017). Flexible piezoelectric films such as PVDF have been explored for use in footwear, prosthetics, and wearable systems, where body movement can sustain low-power electronics (Anton & Sodano, 2007; Pu et al., 2022). Researchers have also investigated piezoelectric materials for medical wearables—for example, using body motion to supplement insulin pump power or extend the lifetime of continuous glucose monitors (Chen et al., 2022; Chorsi et al., 2022). Beyond consumer systems, piezoelectric harvesters have been studied for distributed industrial and infrastructure monitoring, where autonomous nodes can power themselves using machinery vibration or structural oscillation (Sodano et al., 2012). For example, piezoelectric sensors embedded in bridges, buildings, or machinery could monitor structural health by detecting vibrations or stress while simultaneously powering the monitoring system itself, eliminating the need for battery replacement in remote or inaccessible locations.

This experiment investigates the electrical output characteristics of two ceramic piezoelectric discs, 12 mm and 35 mm in diameter, and a flexible PVDF film sensor, all subjected to controlled impact conditions at multiple drop heights (3 cm, 6 cm, 9 cm, and 12 cm). The purpose is to determine how sensor geometry, capacitance, and material flexibility influence voltage generation under consistent mechanical loading. Each sensor was tested under identical conditions using an Arduino Uno R3 for data collection. The analysis focuses on repeatability, reliability, and comparative voltage response across drop heights. The experimental findings contribute to understanding how sensor type and mechanical properties affect instantaneous energy conversion, supporting the optimization of both rigid and flexible piezoelectric systems for small-scale power harvesting and self-powered device design.

### How Piezoelectric Sensors Work

Piezoelectric sensors operate based on the piezoelectric effect, in which certain crystalline or ceramic materials generate an electric voltage when they are mechanically deformed. When stress or pressure is applied, the internal lattice of the material shifts, separating positive and negative charge centers and creating a potential difference across its electrodes. The resulting voltage depends on the rate of strain change rather than the magnitude of static force. Consequently, the rate of force application, rather than the magnitude of static load, determines voltage output. The general relationship between the applied force and the generated voltage can be expressed as:

$$V \propto \frac{d_{33} * \Delta F}{C}$$

where  $d_{33}$  is the piezoelectric charge coefficient,  $\Delta F$  is the change in applied force, and  $C$  is the capacitance of the material. A larger  $d_{33}$  or faster-changing  $\Delta F$  increases voltage, while a higher capacitance smooths and limits it. Typical outputs range from tens of millivolts under gentle pressure to several volts under sharp, impulsive impacts.

Three types of sensors were tested in this study: 12 mm piezo discs, 35 mm piezo discs, and a flexible PVDF film sensor (Figure 1). These sensors were chosen to investigate the tradeoff between rigidity and flexibility for different energy-harvesting and sensing applications. The ceramic discs represent high-output, impact-driven systems, while the PVDF film represents flexible, motion-responsive designs suitable for integration into wearable or structural systems. All sensors were connected to an Arduino Uno R3 for voltage measurement and digital data capture. Because the Arduino's 10-bit analog-to-digital converter (ADC) is limited to a 5 V range, a simple voltage divider circuit was incorporated to accurately measure voltages beyond 5 V and to measure higher outputs without damaging the board. This circuit uses two resistors in series, with the voltage measurement taken at the node between the two resistors, to scale down the input voltage according to the ratio  $V_{out} = V_{in} \times \frac{R_2}{R_2 + R_1}$ , ensuring accurate readings for impacts that generate voltages exceeding the ADC limit.

## Materials and Methods

### Experimental Setup and Equipment

All sensors were connected to an Arduino Uno R3 for voltage measurement and digital data capture. Each piezoelectric element was connected directly to the Arduino's analog input (A0). The center lead of the piezo disc was wired to A0, while the brass ring was connected to

**Figure 1**

*Types of sensors used in this experiment*



*Note.* Flexible PVDF film, 12 mm piezo disc, and 35 mm piezo disc used for comparative testing of voltage output under controlled impact conditions.

ground. The Arduino's INPUT\_PULLUP configuration provided a stable bias voltage of approximately 4.90 V, which served as the baseline reference for all measurements.

Because the Arduino's 10-bit analog-to-digital converter (ADC) is limited to a 5 V range, a voltage divider circuit, consisting of two 1 MΩ resistors connected in series, was positioned between the piezo output and ground, with the Arduino measuring voltage across the lower resistor. This configuration provided a 2:1 voltage division ratio, allowing measurement of piezo outputs up to 10V while keeping the Arduino input safely below 5V. This circuit scales down the input voltage according to the ratio:

$$V_{out} = V_{in} \times \frac{R_2}{R_1 + R_2}$$

ensuring accurate readings for impacts that generate voltages exceeding the ADC limit. By using a breadboard for flexible configuration, each sensor could be easily connected and tested under identical conditions while preventing voltage saturation and protecting the Arduino from overvoltage damage.

A custom Arduino sketch was programmed to capture three key metrics from each impact event: the maximum instantaneous voltage swing ( $\Delta V$ ), the integrated voltage signal (proportional to energy), and the maximum slope (indicating the sharpness of the impact). Data was streamed to the Serial Monitor in CSV format for later analysis.

### Drop Test Procedure

Controlled drops simulated impact forces. Initial tests used improvised objects (a water jug and Chapstick), which were later refined to a pendulum-style setup for more consistent release. Drop heights of 3 cm, 6 cm, 9 cm, and 12 cm were used to represent different levels of impact energy, with a dropped mass of approximately 50 grams. For each condition, 10 replicates were recorded to assess variability. The pendulum-style mechanism ensured consistent impact angle and position across all trials, minimizing experimental variation.

### Repeatability Testing Protocol

To evaluate repeatability, trials were conducted using two separate sensors of the same type under identical conditions. This approach allowed direct comparison between sensors to determine whether similar devices produced consistent outputs when subjected to the same force. For each drop height, both sensors were tested multiple times, and their outputs were compared. This method ensured that observed differences in performance reflected sensor-to-sensor variation rather than inconsistencies in the experimental setup.

### Reliability Testing Protocol

Reliability was assessed by repeatedly testing the same sensor under identical conditions over multiple trials. For each drop height, a single sensor was impacted several times in succession, and its voltage outputs were recorded. By analyzing the variation within these repeated trials, the consistency of a given sensor's response over time could be measured. This procedure allowed evaluation of whether individual sensors could reliably reproduce their performance across multiple uses, an important factor for practical applications.

### Statistical Analysis Methods

To assess whether observed differences between sensors were statistically meaningful, standard deviations were calculated for all test conditions. Coefficients of variation ( $CV = \text{standard deviation} / \text{mean} \times 100\%$ ) were computed to compare relative variability across sensors with different voltage ranges. Analysis of repeatability data across multiple time intervals between drops (1, 5, 10, 15, and 20 seconds) was conducted to evaluate time-dependent drift or settling effects.

Statistical significance of differences was evaluated by comparing the magnitude of voltage differences between sensors to their combined standard deviations. Differences exceeding  $2\times$  the combined standard deviation were considered statistically meaningful, indicating that observed performance variations reflected genuine sensor characteristics rather than measurement noise.

### Limitations

Several sources of experimental uncertainty may have influenced the recorded measurements. The Arduino Uno's 10-bit analog-to-digital converter provides a resolution of approximately 4.9 mV per step ( $5\text{V} \div 1024$ ), which introduces quantization error in all voltage readings. When combined with the voltage divider circuit, this resolution is further reduced by the resistor ratio, potentially limiting the precision of peak voltage measurements. However, given that most voltage swings exceeded 2V, the relative error from ADC quantization remained below 0.5% for the majority of measurements.

Impact angle and contact position consistency represented significant sources of variability. Despite using a pendulum-style release mechanism to improve reproducibility, slight variations in drop trajectory or sensor surface contact could alter the rate of force application and thus the instantaneous voltage spike. The 12 mm sensor's relatively higher trial-to-trial variability (Standard Deviation  $\approx 0.32\text{V}$  at high drops) compared to the larger sensors suggests that smaller contact areas are more sensitive to positioning errors. The PVDF film's flexibility may have actually reduced this sensitivity, as the material conforms more readily to impact variations, potentially explaining its lower standard deviation.

The voltage divider circuit introduces measurement considerations. The two  $1\text{ M}\Omega$  resistors connected in series formed a 2:1 voltage divider, which minimizes current draw from the piezoelectric element. Additionally, the baseline voltage of approximately 4.90V recorded by the Arduino represents the INPUT\_PULLUP bias rather than true ground, meaning all voltage swings are measured relative to this reference. This approach is valid for comparative analysis but means absolute voltage values should be interpreted as voltage changes ( $\Delta V$ ) rather than absolute potentials.

Temperature and humidity were not controlled during testing, and piezoelectric materials can exhibit temperature-dependent behavior. However, all tests were conducted in the same environment over a short time period, minimizing the impact of environmental drift. Future work could incorporate controlled environmental conditions and calibrated force sensors to further reduce measurement uncertainty.

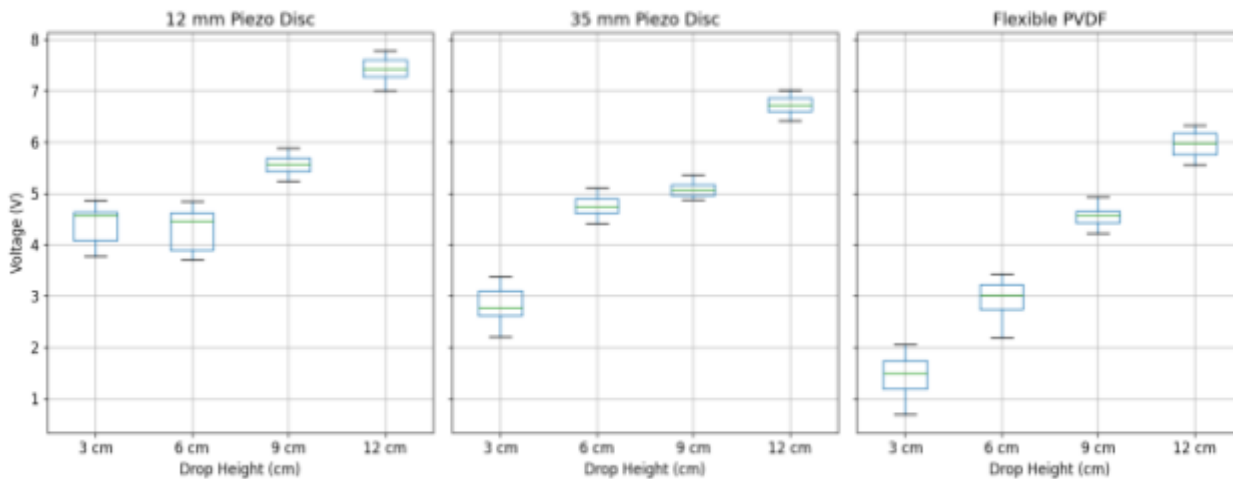
## Results

### Voltage Response Across Drop Heights

Voltage measurements across all three sensors revealed distinct response patterns to increasing drop height. Figure 2 presents the complete dataset for drop heights of 3, 6, 9, and 12 cm. The 12 mm piezo disc generated an average of 3.96V at 3 cm and maintained similar output (3.80V) at 6 cm, indicating minimal response to this modest increase in impact energy. However, at 9 cm and above, voltage output increased substantially, reaching 5.30V and 7.00V at 9 cm and 12 cm, respectively, with individual trials as high as 7.78V. This threshold behavior suggests the smaller disc requires higher impact forces to achieve maximum performance.

The 35 mm piezo disc demonstrated markedly different behavior, showing its strongest relative response at lower impact energies. Output more than doubled from 2.33V at 3 cm to 4.73V at 6 cm, the largest percentage increase observed for any sensor. At higher drops, voltage continued to rise but at a more gradual rate, reaching 5.22V at 9 cm and 6.83V at 12

**Figure 2**  
*Voltage distribution by drop height*



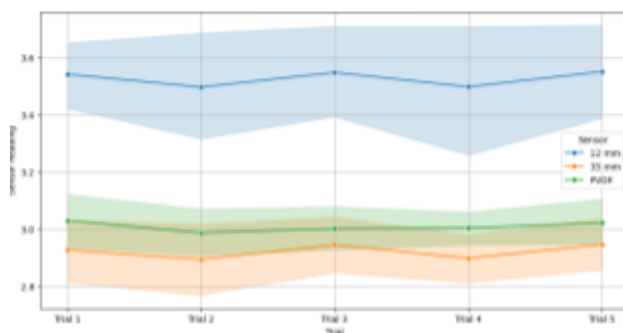
*Note.* Average piezoelectric voltage output vs drop height for all three sensor types: 12 mm disc, 35 mm disc, and flexible PVDF film. Error bars represent one standard deviation across ten trials per height.

cm, with individual trials reaching 7.01V. This pattern indicates greater sensitivity at moderate force levels compared to the smaller disc.

The flexible PVDF film sensor produced the lowest absolute voltages but demonstrated the most linear response profile. Starting below 1.5V at 3 cm, the output increased progressively to approximately 2.8V at 6 cm, 4.6V at 9 cm, and 6.33V at 12 cm. Notably, the PVDF sensor showed consistent, proportional voltage increases across the entire range without the threshold effects observed in the ceramic discs.

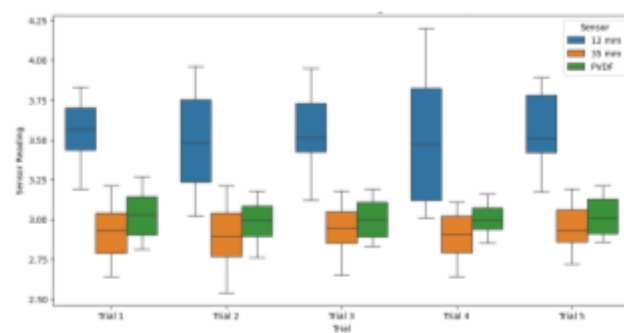
At low impact energies (3 cm), the 12 mm disc produced the highest voltage. However, at 6 cm, the 35 mm disc generated the highest output (~4.7V), surpassing the 12 mm disc (~3.8V). At higher drop heights (9 cm and 12 cm), the 12 mm disc regained dominance, producing the

**Figure 3a**  
*Sensor readings across trials*



*Note.* Repeatability of the 12 mm, 35 mm, and flexible PVDF sensors across five trials at a 3 cm drop height. Shaded regions indicate standard deviation.

**Figure 3b**  
*Distribution sensor readings across trials*



*Note.* Distribution of readings for each sensor across trials, showing variability within and between measurements.



highest voltages of all sensors tested. The PVDF sensor, while producing the lowest voltages overall, demonstrated the most consistent growth across all drop heights.

### Repeatability Analysis

Figures 3a and 3b present repeatability data from trials conducted at 3 cm drop height with varying time intervals between successive impacts (1, 5, 10, 15, and 20 seconds).

All three sensors produced consistent results across repeated drops, confirming high repeatability. The 12 mm disc yielded the highest voltages, followed by the 35 mm and PVDF sensors. Standard deviation bands were narrow, indicating stable behavior, although the 12 mm sensor displayed slightly greater variability, likely due to its rigidity and higher sensitivity to small mechanical differences in impact. The box plots further confirm that median values remained steady, supporting the reliability of the setup and repeatability of measurements under identical conditions.

For the 12 mm sensor tested at 3 cm with varying time delays, mean values ranged only from 3.497 V to 3.591 V, a span of less than 3%. This narrow variation confirms that the sensors do not exhibit time-dependent drift or require settling periods between measurements. Similarly, the 35 mm disc and PVDF sensors maintained consistent outputs across all timing conditions, with coefficient of variation values below 10% in all cases.

### Reliability and Sensor-to-Sensor Variation

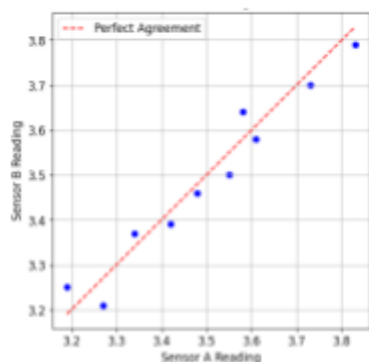
Figures 4a–4c display one-to-one comparisons between paired sensors of each type tested under identical conditions.

The data for all sensors align closely along the line of perfect agreement, indicating strong reliability and minimal measurement deviation between identical units. The 12 mm discs showed the tightest correlation, while the PVDF sensors exhibited slightly greater scatter due to material flexibility. Overall, these plots confirm that each sensor type can be interchanged within the same category without significantly affecting data accuracy.

The 12 mm piezo disc exhibited standard deviations ranging from 0.21 V at 3 cm to approximately 0.32 V at higher drop heights, representing roughly 6–8% of the mean voltage values. The 35 mm disc showed similar relative variability, with standard deviations of

**Figure 4a**

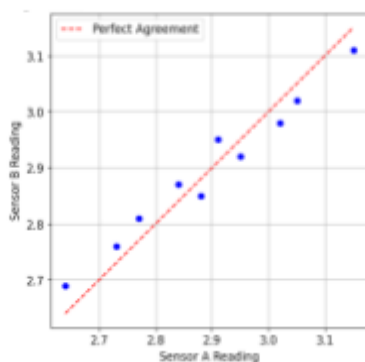
*12mm sensor reliability: sensor A vs. sensor B*



*Note.* Reliability comparison between two identical 12mm piezo discs (Sensor A vs. Sensor B).

**Figure 4b**

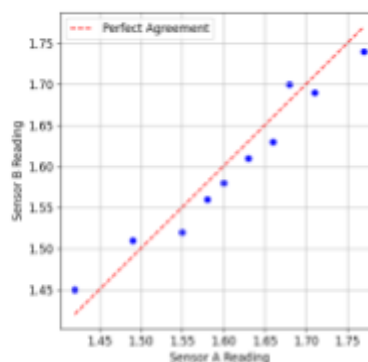
*35mm sensor reliability: sensor A vs. sensor B*



*Note.* Reliability comparison between two identical 35mm piezo discs.

**Figure 4c**

*Flexible Piezo reliability: sensor A vs. sensor B*



*Note.* Reliability comparison between two identical flexible PVDF film sensors.



approximately 0.18V at 3 cm and 0.21 V at higher drops. The PVDF sensor demonstrated the highest consistency, with standard deviations of 0.15 V or lower across all conditions.

The voltage differences between sensors at each drop height exceeded the standard deviations by factors of 2-5X, indicating that observed performance differences are statistically significant rather than artifacts of measurement noise. For example, at 12 cm, the difference between the 12 mm disc (7.00 V) and the 35 mm disc (6.83 V) is small (0.17 V) and within combined measurement uncertainty, suggesting comparable maximum voltage capacity. However, the difference between either ceramic disc and the PVDF sensor (6.33 V) is approximately 0.5-0.7 V, which exceeds the combined standard deviations and represents a meaningful performance distinction.

## Discussion

### Interpretation of Voltage Response Patterns

The observed differences in sensor performance can be attributed to fundamental differences in geometry and material properties. The 12 mm disc, being smaller and stiffer, produced faster voltage spikes that generated outputs exceeding the Arduino Uno's 5 V measurement range during high-energy impacts, necessitating the voltage divider circuit. This behavior reflects its low capacitance and high stiffness, which enables rapid charge accumulation but limits total energy storage. The 35 mm disc, with a larger surface area and higher capacitance, produced smoother voltage responses with slightly lower peaks. Although capable of storing more charge, its slower deformation rate limits instantaneous voltage rise. The flexible PVDF film sensor, composed of a polymer material, demonstrated high flexibility and motion sensitivity but consistently lower voltages due to its small charge constant and low modulus.

The distinct voltage response patterns observed across the three sensor types reflect fundamental differences in their electromechanical properties and geometry. The 12 mm disc's threshold behavior, minimal response at low drops (3-6 cm) followed by dramatic increases at higher energies, suggests that smaller piezoelectric elements require a minimum energy threshold to overcome internal capacitance effects and generate measurable voltage changes. Below this threshold, the rate of charge dissipation through internal capacitance approaches the rate of charge generation, limiting net voltage accumulation.

The 35 mm disc's performance at moderate impact energies (6 cm drops) indicates that larger surface area sensors achieve better electromechanical coupling at lower strain rates. The doubling of voltage output between 3 and 6 cm drops demonstrates high sensitivity in this regime, making larger discs more suitable for ambient vibration harvesting, where forces are frequent but less intense. However, the convergence of voltage outputs between the 12 mm and 35 mm discs at the highest drop height (7.00V vs 6.83V) suggests that both ceramic sensors approach similar maximum polarization limits when subjected to high-energy impacts.

The PVDF film's linear response across all drop heights indicates that polymeric piezoelectric materials, despite lower absolute voltage outputs, provide more predictable performance across a wider dynamic range. This characteristic may be advantageous in applications requiring consistent signal processing without complex calibration or threshold detection. The film's flexibility also appears to reduce sensitivity to impact position variations, as evidenced by its lower standard deviations compared to the rigid ceramic discs.

### Comparison with Piezoelectric Theory

These results align with established piezoelectric theory, which predicts that voltage output depends on the rate of strain change ( $d\epsilon/dt$ ) rather than static load magnitude. The

relationship  $V \propto (d_{33} \times \Delta F) / C$  explains why the 12 mm disc, with its lower capacitance, generates higher peak voltages under rapid impacts despite having a smaller surface area. Conversely, the 35 mm disc's higher capacitance smooths voltage transients but enables greater total charge storage, consistent with the charge equation  $Q = C \times V$ .

Initially, it was hypothesized that placing a heavier object on the sensor would yield higher voltages, since greater weight would apply more force. However, through both background research and experimental testing, this assumption was found to be incorrect. When weight is applied slowly, the piezo element deforms gradually, allowing charges to dissipate through its internal capacitance before a strong potential can build up. In contrast, a quick or sharp impact changes the strain much faster, causing a large, brief voltage spike. The experimental results confirmed this: dropping an object from a higher height (which increases the rate of impact) produced significantly higher voltage readings, while simply increasing the weight with slow pressure produced little to no additional voltage.

The PVDF film's behavior reflects its lower piezoelectric charge coefficient ( $d_{33} \approx 20\text{-}30$  pC/N) compared to ceramic materials ( $d_{33} \approx 200\text{-}400$  pC/N), explaining its consistently lower voltage outputs. However, PVDF's flexibility and lower elastic modulus allow it to achieve comparable strain magnitudes under lower applied forces, partially compensating for its lower charge coefficient in flexible applications.

### **Practical Implications for Sensor Selection**

The findings of this study have direct implications for piezoelectric sensor selection in energy harvesting and sensing applications. A few key examples are: High-energy impact detection: The 12 mm disc's threshold behavior and high peak voltages make it ideal for applications requiring force discrimination. For example, it could be integrated into door security systems that trigger alerts only when struck with sufficient force, filtering out accidental bumps or light touches. Similarly, it could serve in quality control systems detecting defective products through impact testing, or in automotive crash sensors requiring instantaneous high-voltage signals.

Moderate-energy harvesting: The 35 mm disc's sensitivity at moderate impact forces makes it suitable for continuous energy harvesting from ambient vibrations. It could power remote environmental sensors in locations like forests or offshore platforms where consistent vibrations from wind or waves provide steady energy input. Urban applications could include sidewalk or roadway installations harvesting pedestrian or vehicular traffic energy.

Flexible, distributed sensing: The PVDF film's linear response, flexibility, and consistency make it optimal for wearable and structural monitoring. It could be woven into athletic clothing to power biometric sensors tracking heart rate and movement during exercise, integrated into prosthetic limbs to provide feedback about ground contact forces, or embedded in aircraft wings or bridge structures to monitor strain and vibration patterns continuously.

### **Study Limitations & Future Research Directions**

Several limitations of this study should be acknowledged. First, the experiment focused exclusively on instantaneous voltage response rather than power output or energy conversion efficiency over time. While peak voltage is important for triggering electronics, practical energy harvesting applications require sustained power delivery, necessitating integration of voltage outputs over extended periods and consideration of impedance matching to load circuits.

Second, the controlled drop test, while providing excellent repeatability, does not fully replicate the complex loading conditions encountered in real-world applications. Actual vibrations typically exhibit sinusoidal or random patterns rather than discrete impacts, and the

frequency content of vibrations significantly affects piezoelectric response. Testing under realistic vibration profiles would provide more directly applicable performance data.

Third, no power conditioning circuitry was employed in this study. Practical energy harvesting systems require rectification, voltage regulation, and energy storage components that introduce additional losses and complexity. The usable energy from these sensors would be lower than suggested by peak voltage measurements alone.

Finally, long-term durability testing was not conducted. Piezoelectric materials can exhibit performance degradation through mechanical fatigue, depolarization, or environmental exposure. Understanding the operational lifetime of these sensors under repeated impact conditions would be essential for deployment in permanent installations.

Future work could address these limitations through several avenues of investigation, namely studying energy conversion efficiency, frequency response characterization, power conditioning integration, hybrid sensor arrays, environmental durability, and real-world deployment. By measuring power output over time and connecting sensors to known resistive loads, one could measure realistic estimates of harvestable energy under different loading conditions. Additionally, testing sensors under sinusoidal vibration inputs across a range of frequencies (1-1000 Hz) would identify optimal operating conditions for different vibration environments. To evaluate end-to-end system efficiency, a complete energy harvesting circuit, incorporating rectifiers, voltage regulators, and storage capacitors or rechargeable batteries, could be developed. Combinations of different sensor types (e.g., small discs for peak detection with large discs for energy harvesting) could optimize both signal quality and power generation simultaneously. Aging studies would expose sensors to extended cycling, temperature variations, humidity, and mechanical stress to assess long-term reliability and predict operational lifetimes. Finally, deploying sensors in actual application environments (e.g., building floors, machinery, wearable devices) could validate laboratory findings and identify challenges in practical implementation.

### Conclusions

This work demonstrated that each sensor type has distinct strengths and is best suited to specific applications based on its voltage response characteristics, sensitivity profile, and mechanical properties. Overall, the 12 mm disc suits fast-response detection, the 35 mm disc fits energy-harvesting systems, and the PVDF film excels in flexible, motion-sensitive environments. The results of this experiment demonstrate that different piezoelectric sensor geometries exhibit distinct performance characteristics, suggesting that sensor selection should be matched to specific application requirements. Statistical analysis confirmed that observed performance differences are meaningful and reproducible, with coefficients of variation below 10% for all sensor types. These findings contribute to the growing body of research supporting the potential of piezoelectric materials in self-powered and adaptive technologies, providing quantitative performance data to guide sensor selection for energy harvesting and sensing applications.

## References

- S. Roundy, P. K. Wright, and J. Rabaey, "Energy scavenging for wireless sensor networks with special focus on vibrations," *Proc. IEEE*, vol. 96, no. 9, pp. 1457-1486, Sept. 2008. <https://doi.org/10.1109/JPROC.2007.908052>
- Maghsoud, R., "Advantages, Limitations, and Industrial Applications of Lithium-Ion Batteries," in *Piezoelectricity and Piezoelectric Materials*, Wiley-VCH, 2023, ch. 22. <https://doi.org/10.1002/9783527838851.ch22>
- J. G. Rocha, L. M. Goncalves, P. F. Rocha, M. P. Silva, and S. Lanceros-Mendez, "Energy harvesting from piezoelectric materials fully integrated in footwear," *IEEE Trans. Ind. Electron.*, vol. 57, no. 3, pp. 813-819, Mar. 2010. <https://doi.org/10.1109/TIE.2009.2028360>
- C. A. Howells, "Piezoelectric energy harvesting," *Energy Convers. Manage.*, vol. 50, no. 7, pp. 1847-1850, July 2009. <https://doi.org/10.1016/j.enconman.2009.02.020>
- F. Laumann, M. M. Sørensen, R. F. Jul Lindemann, T. M. Hansen, and T. Tambo, "Energy harvesting through piezoelectricity - technology foresight," *Energy Procedia*, vol. 142, pp. 3062-3068, Dec. 2017. <https://doi.org/10.1016/j.egypro.2017.12.445>
- A. Nechibvute, A. Chawanda, and P. Luhanga, "Piezoelectric energy harvesting devices: An alternative energy source for wireless sensors," *Smart Mater. Res.*, vol. 2012, Article ID 853481, 13 pages, 2012. <https://doi.org/10.1155/2012/853481>
- Z. Yang, L. Dong, M. Wang, G. Liu, X. Li, and Y. Li, "A wearable insulin delivery system based on a piezoelectric micropump," *Sens. Actuators A*, vol. 347, Article 113909, Nov. 2022. <https://doi.org/10.1016/j.sna.2022.113909>
- Z. Yi, W. M. Zhang, and B. Yang, "Piezoelectric approaches for wearable continuous blood pressure monitoring: a review," *J. Micromech. Microeng.*, vol. 32, no. 10, Article 103003, Oct. 2022. <https://doi.org/10.1088/1361-6439/ac87ba>

## Appendix

### Arduino Data Acquisition Code

The following Arduino sketch was developed to capture voltage data from piezoelectric sensors during impact testing. The code implements a state machine with three states (IDLE, CAPTURE, REFRACTORY) to detect impact events, record voltage transients, and prevent multiple triggers from a single impact. Key features include oversampling for noise reduction, baseline tracking, and calculation of multiple metrics: peak voltage swing ( $\Delta V$ ), integrated area under the voltage curve (proportional to energy), and maximum slope (indicating impact sharpness).

```
/*
  Piezo single-shot logger (downward swing only) with area & slope
  Wiring: piezo + (center) -> A0, piezo - (brass) -> GND
  CSV: sensor_id,force_label,deltaV_down_V,area_Vs,maxSlope_Vps,
      minV_V,baseline_V,duration_ms,samples,clipped
*/
const int  PIEZO = A0;
const float VREF  = 5.0;
const float ADC_LSB = VREF / 1023.0;
String SENSOR_ID  = "Sensor_1";
String FORCE_LABEL = "50_grams"; // use for your test label
// Tuning
const unsigned long SAMPLE_US  = 500; // ~2 kHz
const float THRESHOLD_DOWN_V  = 0.10; // raise if too sensitive
const float BASELINE_ALPHA_IDLE = 0.001; // slow EMA when idle
const int  CAPTURE_MS        = 140; // capture window
const int  REFRACTORY_MS     = 1000; // lockout after capture
const float RETURN_BAND_V    = 0.02; // re-arm band
const int  OVERSAMPLE_N      = 4;
enum State { IDLE, CAPTURE, REFRACTORY };
State state = IDLE;
unsigned long tStateStart = 0, lastSample = 0;
float baseline = 0.0;
float minV = 5.0;
unsigned long nSamples = 0;
bool clipped = false;
// New metrics
float area_Vs = 0.0; // integral of (baseline - v) when positive
float maxSlope_Vps = 0.0; // most negative dV/dt (downward), in V/s
float prevV = 5.0;

float readSmoothedV() {
  long acc = 0;
  for (int i = 0; i < OVERSAMPLE_N; i++) acc += analogRead(PIEZO);
  return (float)acc / OVERSAMPLE_N * ADC_LSB;
}
```

```
void setup() {
  Serial.begin(115200);
  pinMode(PIEZO, INPUT_PULLUP);
  delay(80);
  float acc = 0;
  for (int i = 0; i < 80; i++) { acc += analogRead(PIEZO); delay(2); }
  baseline = (acc / 80.0) * ADC_LSB;
  prevV = baseline;
  Serial.println("sensor_id,force_label,deltaV_down_V,area_Vs,maxSlope_Vps,minV_V,baseline_
V,duration_ms,samples,clipped");
}
void loop() {
  unsigned long now = micros();
  if (now - lastSample < SAMPLE_US) return;
  unsigned long dt_us = now - lastSample;
  lastSample = now;
  float v = readSmoothedV();
  switch (state) {
    case IDLE: {
      baseline += BASELINE_ALPHA_IDLE * (v - baseline);
      float drop = baseline - v;
      if (drop >= THRESHOLD_DOWN_V) {
        state = CAPTURE;
        tStateStart = millis();
        minV = v;
        nSamples = 1;
        clipped = false;
        area_Vs = 0.0;
        maxSlope_Vps = 0.0;
      }
      break;
    }
    case CAPTURE: {
      nSamples++;
      if (v < minV) minV = v;
      // bottom-rail clip only
      if (v <= 0.02) clipped = true;
      // integrate downward swing (only if below baseline)
      float drop = baseline - v;
      if (drop > 0) area_Vs += drop * (dt_us / 1e6f);
      // slope (V/s), downward is negative; we report magnitude
      float slope = (v - prevV) / (dt_us / 1e6f);
      float downSlopeMag = slope < 0 ? -slope : 0;
      if (downSlopeMag > maxSlope_Vps) maxSlope_Vps = downSlopeMag;

      if ((millis() - tStateStart) >= CAPTURE_MS) {
```



```
float deltaDown = baseline - minV;
unsigned long duration_ms = CAPTURE_MS;
Serial.print(SENSOR_ID); Serial.print(",");
Serial.print(FORCE_LABEL); Serial.print(",");
Serial.print(deltaDown, 4); Serial.print(",");
Serial.print(area_Vs, 6); Serial.print(",");
Serial.print(maxSlope_Vps, 2); Serial.print(",");
Serial.print(minV, 4); Serial.print(",");
Serial.print(baseline, 4); Serial.print(",");
Serial.print(duration_ms); Serial.print(",");
Serial.print(nSamples); Serial.print(",");
Serial.println(clipped ? "CLIPPED" : "OK");
state = REFRACTORY;
tStateStart = millis();
}
break;
}
case REFRACTORY: {
  bool timeUp = (millis() - tStateStart) >= REFRACTORY_MS;
  bool quiet = fabs(baseline - v) < RETURN_BAND_V;
  if (timeUp && quiet) state = IDLE;
  break;
}
}
prevV = v;
}
```

### Code Description:

This Arduino sketch operates as a triggered data acquisition system for piezoelectric impact testing. The program continuously monitors the analog input (A0) at approximately 2 kHz sampling rate and maintains a slow-moving average baseline voltage representing the sensor's rest state.

When an impact occurs, the voltage drops below baseline by more than the threshold (0.10V), triggering the CAPTURE state. During the 140-ms capture window, the code records:

- **Minimum voltage (minV)**: The lowest voltage reached during impact
- **Voltage swing ( $\Delta V$ )**: Calculated as baseline - minV
- **Integrated area (area\_Vs)**: The time integral of voltage deviation, proportional to total energy
- **Maximum slope (maxSlope\_Vps)**: The steepest rate of voltage change, indicating impact sharpness

After capture, the system enters a 1-second REFRACTORY period to prevent re-triggering on the same impact event. The system only returns to IDLE when both the refractory timeout expires and the sensor voltage returns close to baseline, ensuring clean separation between successive impacts.

Data output is formatted as comma-separated values (CSV) for easy import into a spreadsheet or analysis software, with each line representing one complete impact event.



## Acknowledgements

I would like to express my sincere gratitude to my mentor, Veronica Contreras, for her invaluable guidance and support throughout this research project. Her expertise, patience, and encouragement were instrumental in helping me navigate the challenges of experimental design, data analysis, and scientific writing.

I am deeply grateful to my father for making this work possible by providing the materials and equipment necessary to conduct these experiments. His technical knowledge and willingness to help whenever I encountered difficulties were essential to the successful completion of this study.